Article

Site-Specific Interactions of Cu(II) with # and #-Synuclein: Bridging the Molecular Gap between Metal Binding and Aggregation

Andre#s Binolfi, Gonzalo R. Lamberto, Rosario Duran, Liliana Quintanar, Carlos W. Bertoncini, Jose M. Souza, Carlos Cerven#ansky, Markus Zweckstetter, Christian Griesinger, and Claudio O. Ferna#ndez

J. Am. Chem. Soc., **2008**, 130 (35), 11801-11812 • DOI: 10.1021/ja803494v • Publication Date (Web): 09 August 2008

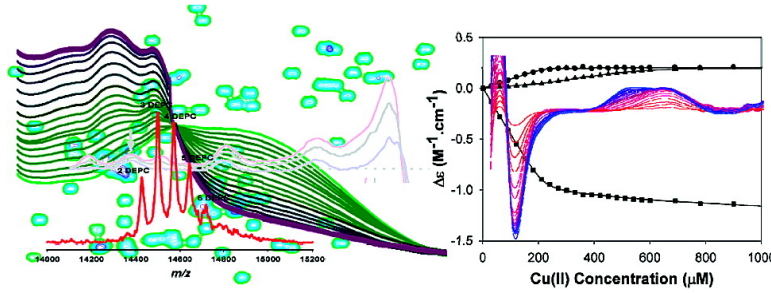

More About This Article

Additional resources and features associated with this article are available within the HTML version:

- Supporting Information
- Access to high resolution figures
- Links to articles and content related to this article
- Copyright permission to reproduce figures and/or text from this article

View the Full Text HTML

J|A|C|S
ARTICLES

Published on Web 08/09/2008

Site-Specific Interactions of Cu(II) with α and β-Synuclein: Bridging the Molecular Gap between Metal Binding and Aggregation

Andrés Binolfi,[†] Gonzalo R. Lamberto,[†] Rosario Duran,[‡] Liliana Quintanar,[§] Carlos W. Bertoncini,[||] Jose M. Souza,[⊥] Carlos Cerveñansky,[‡] Markus Zweckstetter,[#,▽] Christian Griesinger,[#,▽] and Claudio O. Fernández*[,†,#]

Instituto de Biología Molecular y Celular de Rosario, Consejo Nacional de Investigaciones Científicas y Técnicas, Universidad Nacional de Rosario, Suipacha 531, S2002LRK Rosario, Argentina, Institut Pasteur de Montevideo e Instituto de Investigaciones Biológicas Clemente Estable, Calle Mataojo 2020, 11400 Montevideo, Uruguay, Departamento de Química, Centro de Investigación y Estudios Avanzados (Cinvestav), Av. Instituto Politécnico Nacional 2508, 07360 D.F., México, Department of Chemistry, University of Cambridge, Lensfield Road, Cambridge CB2 1EW, United Kingdom, Departamento de Bioquímica, Facultad de Medicina, Universidad de la República, Av. Gral. Flores 2125, 11800 Montevideo, Uruguay, Department of NMR-Based Structural Biology, Max Planck Institute for Biophysical Chemistry, Am Fassberg 11, D-37077 Göttingen, Germany, and DFG Research Center for the Molecular Physiology of the Brain (CMPB), 37073 Göttingen, Germany

Received May 10, 2008; E-mail: cfernan@gwdg.de

Abstract: The aggregation of α-synuclein (AS) is a critical step in the etiology of Parkinson's disease (PD) and other neurodegenerative synucleinopathies. Protein−metal interactions play a critical role in AS aggregation and might represent the link between the pathological processes of protein aggregation and oxidative damage. Our previous studies established a hierarchy in AS−metal ion interactions, where Cu(II) binds specifically to the protein and triggers its aggregation under conditions that might be relevant for the development of PD. In this work, we have addressed unresolved structural details related to the binding specificity of Cu(II) through the design of site-directed and domain-truncated mutants of AS and by the characterization of the metal-binding features of its natural homologue β-synuclein (BS). The structural properties of the Cu(II) complexes were determined by the combined application of nuclear magnetic resonance, electron paramagnetic resonance, UV−vis, circular dichroism spectroscopy, and matrix-assisted laser desorption ionization mass spectrometry (MALDI MS). Two independent, noninteracting copper-binding sites with significantly different affinities for the metal ion were detected in the N-terminal regions of AS and BS. MALDI MS provided unique evidence for the direct involvement of Met1 as the primary anchoring residue for Cu(II) in both proteins. Comparative spectroscopic analysis of the two proteins allowed us to deconvolute the Cu(II) binding modes and unequivocally assign the higher-affinity site to the N-terminal amino group of Met1 and the lower-affinity site to the imidazol ring of the sole His residue. Through the use of competitive chelators, the affinity of the first equivalent of bound Cu(II) was accurately determined to be in the submicromolar range for both AS and BS. Our results prove that Cu(II) binding in the C-terminal region of synucleins represents a nonspecific, very low affinity process. These new insights into the bioinorganic chemistry of PD are central to an understanding of the role of Cu(II) in the fibrillization process of AS and have implications for the molecular mechanism by which BS might inhibit AS amyloid assembly.

Introduction

Parkinson's disease (PD), the second most common neurodegenerative disorder, is associated with the degeneration of dopaminergic neurons in the substantia nigra pars compacta.[1] One of the pathological hallmarks of PD and related synucleinopathies is the presence of intracellular inclusions called Lewy bodies that consist of aggregates of the presynaptic soluble protein α-synuclein (AS).[2,3] Since this discovery, the process of AS aggregation has been proposed to underlie dopaminergic degeneration in PD.[3] Therefore, delineating the mechanism of

[†] Universidad Nacional de Rosario.
[‡] Institut Pasteur de Montevideo e Instituto de Investigaciones Biológicas Clemente Estable.
[§] Centro de Investigación y Estudios Avanzados.
[||] University of Cambridge.
[⊥] Universidad de la República.
[#] Max Planck Institute for Biophysical Chemistry.
[▽] DFG Research Center for the Molecular Physiology of the Brain.

(1) Forno, L. S. *J. Neuropathol. Exp. Neurol.* **1996**, *55*, 259–272.
(2) Spillantini, M. G.; Schmidt, M. L.; Lee, V. M.; Trojanowski, J. Q.; Jakes, R.; Goedert, M. *Nature* **1997**, *388*, 839–840.
(3) Goedert, M. *Nat. Rev. Neurosci.* **2001**, *2*, 492–501.

AS aggregation and its pathophysiological role in neurodegeneration has been the focus of many investigations.[4−7]

Structurally, AS comprises 140 amino acids distributed in three different regions: the amphipathic N-terminus (residues 1−60), showing the consensus repeats KTKEGV and involved in lipid binding; the highly hydrophobic, self-aggregating sequence known as NAC (residues 61−95), which is presumed to initiate fibrillation;[8] and the acidic C-terminal region (residues 96−140), which is rich in Pro, Asp, and Glu residues and critical for blocking rapid AS filament assembly.[4,6] In its native monomeric state, AS adopts an ensemble of conformations with no rigid secondary structure, although long-range interactions have been shown to stabilize an aggregation-autoinhibited conformation.[9−14] The precise function of AS is unknown, as are the mechanism(s) underlying the structural transition from the innocuous, monomeric conformations of AS to its neurotoxic forms.

There is now increasing evidence that altered metal homeostasis may be involved in the progression of neurodegenerative diseases.[15−19] Protein−metal interactions appear to play a critical role in protein aggregation and are therefore likely to provide a link between the accumulation of aggregated proteins, oxidative damage of the brain, and neuronal cell loss.[20−24] Interestingly, copper has been implicated in Creutzfeldt−Jakob disease,[25−28] whereas recent studies emphasize the role of copper, iron, and zinc as contributors to both amyloid Aβ assembly in vitro and the neuropathology of Alzheimer's disease (AD).[25,29−34] High levels of copper, zinc, and iron were also found in and around amyloid plaques of AD brains.[35] Furthermore, coordination environments for Cu(II) complexes in the amyloid precursor protein, the amyloid Aβ peptide, and the prion protein have been very well characterized by several biophysical and structural studies.[28,34,36−46] Detailed knowledge of the structural and binding features of relevant metal ions as well as the mechanism by which these metal ions might participate in the fibrillization of these proteins has contributed to the design of a new therapeutical scheme based on the development of metal ion chelators.[17,19]

The role of metal ions in AS amyloid assembly and neurodegeneration is also becoming a central question in the pathophysiology of PD. Iron deposits have been identified in Lewy bodies in the substantia nigra,[47] and elevated copper concentrations have been reported in the cerebrospinal fluid of PD patients.[48] In addition, individuals with chronic industrial exposure to copper, manganese, or iron have an increased rate

(4) Fernandez, C. O.; Hoyer, W.; Zweckstetter, M.; Jares-Erijman, E. A.; Subramaniam, V.; Griesinger, C.; Jovin, T. M. *EMBO J.* **2004**, *23*, 2039–2046.
(5) Hoyer, W.; Antony, T.; Cherny, D.; Heim, G.; Jovin, T. M.; Subramaniam, V. *J. Mol. Biol.* **2002**, *322*, 383–393.
(6) Hoyer, W.; Cherny, D.; Subramaniam, V.; Jovin, T. M. *Biochemistry* **2004**, *43*, 16233–16242.
(7) Volles, M. J.; Lansbury, P. T., Jr *Biochemistry* **2003**, *42*, 7871–7878.
(8) Giasson, B. I.; Murray, I. V.; Trojanowski, J. Q.; Lee, V. M. *J. Biol. Chem.* **2001**, *276*, 2380–2386.
(9) Bertoncini, C. W.; Jung, Y. S.; Fernandez, C. O.; Hoyer, W.; Griesinger, C.; Jovin, T. M.; Zweckstetter, M. *Proc. Natl. Acad. Sci. U.S.A.* **2005**, *102*, 1430–1435.
(10) Lee, J. C.; Langen, R.; Hummel, P. A.; Gray, H. B.; Winkler, J. R. *Proc. Natl. Acad. Sci. U.S.A.* **2004**, *101*, 16466–16471.
(11) Lee, J. C.; Gray, H. B.; Winkler, J. R. *J. Am. Chem. Soc.* **2005**, *127*, 16388–16389.
(12) Lee, J. C.; Lai, B. T.; Kozak, J. J.; Gray, H. B.; Winkler, J. R. *J. Phys. Chem. B.* **2007**, *111*, 2107–2112.
(13) Dedmon, M. M.; Lindorff-Larsen, K.; Christodoulou, J.; Vendruscolo, M.; Dobson, C. M. *J. Am. Chem. Soc.* **2005**, *127*, 476–477.
(14) Bertoncini, C. W.; Fernandez, C. O.; Griesinger, C.; Jovin, T. M.; Zweckstetter, M. *J. Biol. Chem.* **2005**, *280*, 30649–30652.
(15) Bush, A. I. *Curr. Opin. Chem. Biol.* **2000**, *4*, 184–191.
(16) Sayre, L. M.; Perry, G.; Smith, M. A. *Curr. Opin. Chem. Biol.* **1999**, *3*, 220–225.
(17) Gaeta, A.; Hider, R. C. *Br. J. Pharmacol.* **2005**, *146*, 1041–1059.
(18) Kozlowski, H.; Brown, D. R.; Valensin, G. *Metallochemistry of Neurodegeneration: Biological, Chemical and Genetic Aspects; RSC Publishing:* Cambridge, U.K. 2006.
(19) Molina-Holgado, F.; Hider, R. C.; Gaeta, A.; Williams, R.; Francis, P. *Biometals* **2007**, *20*, 639–654.
(20) Uversky, V. N.; Li, J.; Fink, A. L. *J. Biol. Chem.* **2001**, *276*, 44284–44296.
(21) Paik, S. R.; Shin, H. J.; Lee, J. H.; Chang, C. S.; Kim, J. *Biochem. J.* **1999**, *340*, 821–828.
(22) Atwood, C. S.; Moir, R. D.; Huang, X. D.; Scarpa, R. C.; Bacarra, N. M. E.; Romano, D. M.; Hartshorn, M. K.; Tanzi, R. E.; Bush, A. I. *J. Biol. Chem.* **1998**, *273*, 12817–12826.
(23) Paik, S. R.; Shin, H. J.; Lee, J. H. *Arch. Biochem. Biophys.* **2000**, *378*, 269–277.
(24) Requena, J. R.; Groth, D.; Legname, G.; Stadtman, E. R.; Prusiner, S. B.; Levine, R. L. *Proc. Natl. Acad. Sci. U.S.A.* **2001**, *98*, 7170–7175.
(25) Brown, D. R.; Kozlowski, H. *Dalton Trans.* **2004**, 1907–1917.
(26) Kim, N. H.; Choi, J. K.; Jeong, B. H.; Kim, J. I.; Kwon, M. S.; Carp, R. I.; Kim, S. *FASEB J.* **2005**, *19*, 783–785.
(27) Gaggelli, E.; Bernardi, F.; Molteni, E.; Pogni, R.; Valensin, D.; Valensin, G.; Remelli, M.; Luczkowski, M.; Kozlowski, H. *J. Am. Chem. Soc.* **2005**, *127*, 996–1006.
(28) Klewpatinond, M.; Davies, P.; Bowen, S.; Brown, D. R.; Viles, J. H. *J. Biol. Chem.* **2008**, *283*, 1870–1881.
(29) Miura, T.; Suzuki, K.; Kohata, N.; Takeuchi, H. *Biochemistry* **2000**, *39*, 7024–7031.
(30) Garzon-Rodriguez, W.; Yatsimirsky, A. K.; Glabe, C. G. *Bioorg. Med. Chem. Lett.* **1999**, *9*, 2243–2248.
(31) Huang, X.; et al. *J. Biol. Chem.* **1999**, *274*, 37111–37116.
(32) Bush, A. I.; Multhaup, G.; Moir, R. D.; Williamson, T. G.; Small, D. H.; Rumble, B.; Pollwein, P.; Beyreuther, K.; Masters, C. L. *J. Biol. Chem.* **1993**, *268*, 16109–16112.
(33) Syme, C. D.; Viles, J. H. *Biochim. Biophys. Acta* **2006**, *1764*, 246–256.
(34) Karr, J. W.; Szalai, V. A. *Biochemistry* **2008**, *47*, 5006–5016.
(35) Lovell, M. A.; Robertson, J. D.; Teesdale, W. J.; Campbell, J. L.; Markesbery, W. R. *J. Neurol. Sci.* **1998**, *158*, 47–52.
(36) Aronoff-Spencer, E.; Burns, C. S.; Avdievich, N. I.; Gerfen, G. J.; Peisach, J.; Antholine, W. E.; Ball, H. L.; Cohen, F. E.; Prusiner, S. B.; Millhauser, G. L. *Biochemistry* **2000**, *39*, 13760–13771.
(37) Chattopadhyay, M.; Walter, E. D.; Newell, D. J.; Jackson, P. J.; Aronoff-Spencer, E.; Peisach, J.; Gerfen, G. J.; Bennett, B.; Antholine, W. E.; Millhauser, G. L. *J. Am. Chem. Soc.* **2005**, *127*, 12647–12656.
(38) Garnett, A. P.; Viles, J. H. *J. Biol. Chem.* **2003**, *278*, 6795–6802.
(39) Barnham, K. J.; McKinstry, W. J.; Multhaup, G.; Galatis, D.; Morton, C. J.; Curtain, C. C.; Williamson, N. A.; White, A. R.; Hinds, M. G.; Norton, R. S.; Beyreuther, K.; Masters, C. L.; Parker, M. W.; Cappai, R. *J. Biol. Chem.* **2003**, *78*, 17401–17407.
(40) Karr, J. W.; Akintoye, H.; Kaupp, L. J.; Szalai, V. A. *Biochemistry* **2005**, *44*, 5478–5487.
(41) Karr, J. W.; Kaupp, L. J.; Szalai, V. A. *J. Am. Chem. Soc.* **2004**, *126*, 13534–13538.
(42) Belosi, B.; Gaggelli, E.; Guerrini, R.; Kozlowski, H.; Luczkowski, M.; Mancini, F. M.; Remelli, M.; Valensin, D.; Valensin, G. *ChemBioChem* **2004**, *5*, 349–359.
(43) Valensin, D.; Luczkowski, M.; Mancini, F. M.; Legowska, A.; Gaggelli, E.; Valensin, G.; Rolka, K.; Kozlowski, H. *Dalton Trans.* **2004**, 1284–1293.
(44) Valensin, D.; Mancini, F. M.; Luczkowski, M.; Janicka, A.; Wisniewska, K.; Gaggelli, E.; Valensin, G.; Lankiewicz, L.; Kozlowski, H. *Dalton Trans.* **2004**, 16–22.
(45) Kowalik-Jankowska, T.; Ruta, M.; Wisniewska, K.; Lankiewicz, L. *J. Inorg. Biochem.* **2003**, *95*, 270–282.
(46) Berti, F.; Gaggelli, E.; Guerrini, R.; Janicka, A.; Kozlowski, H.; Legowska, A.; Miecznikowska, H.; Migliorini, C.; Pogni, R.; Remelli, M.; Rolka, K.; Valensin, D.; Valensin, G. *Chem.−Eur. J.* **2007**, *13*, 1991–2001.
(47) Castellani, R. J.; Siedlak, S. L.; Perry, G.; Smith, M. A. *Acta Neuropathol.* **2000**, *100*, 111–114.
(48) Pall, H. S.; Blake, D. R.; Gutteridge, J. M.; Williams, A. C.; Lunec, J.; Hall, M.; Taylor, A. *Lancet* **1987**, *330*, 238–241.

Figure 1. Alignment of the AS and BS amino acid sequences, displaying the absence of the central hydrophobic NAC region in BS and a shorter C-terminus in AS. Letters shaded in blue indicate amino acids that are different in the two proteins. Histidine residues are highlighted in green.

of PD,[49] whereas metal ions such as aluminum, copper, and iron have been shown to bind AS and accelerate its fibrillation in vitro.[20,50−52] The lack of experimental evidence proving a relationship between metal-binding affinity and aggregation enhancement prompted us to perform a detailed structural characterization of metal−AS interactions. In that work, we showed that Cu(II) binds specifically to AS and is effective in accelerating aggregation at physiologically relevant concentrations.[53] NMR mapping revealed that the most affected regions were located at the N-terminus, comprising the stretch of residues ^{3}VFMKGLS^{9} and the His within the sequence ^{48}VVHGV^{52},[53] in line with several studies supporting a role for His residues as metal-anchoring sites in other amyloidogenic proteins.[36−46] A clear effect was also observed at the C-terminus of AS, ^{119}DPDNEA^{124}, but only at higher Cu(II) concentrations. A comparative analysis with other divalent metal ions revealed a selective effect of AS−metal interactions on AS aggregation kinetics, dictated by structural factors corresponding to different protein domains.[54]

Advances in the bioinorganic chemistry of PD require the details of binding specificity of Cu(II) to AS to be known (i.e., the identity of the high-affinity binding site and the nature of the anchoring residues) and the mechanism through which the metal ion participates in fibrillization events to be better understood. To address such important, unresolved issues, we designed site-directed and domain-truncated mutants of AS and performed comparative experiments on the nonamyloidogenic AS homologue β-synuclein (BS). The structural and dynamic properties of BS in solution have been elucidated recently by us and others using NMR spectroscopy,[55,56] whereas its metal-binding features have remained unexplored. The protein BS constitutes a useful and naturally occurring model for understanding the structural factors modulating Cu(II) binding to AS and elucidating details of the binding sites in the full-length protein, for the following reasons: (1) BS shows a high degree of homology with AS, particularly at the N-terminal region,[57] where specific Cu(II) binding occurs (Figure 1); (2) the sole His residue is shifted from position 50 in AS to position 65 in BS; (3) BS lacks the long-range interactions involving N- and C-terminus and NAC and C-terminus contacts, respectively, that are present in AS;[55] and (4) BS lacks the central hydrophobic NAC sequence, a region that does not bind Cu(II) in AS, rendering the protein nonamyloidogenic and therefore avoiding experimental problems derived from protein aggregation. Besides the sequence homology, BS was shown to be colocalized with AS at the presynaptic terminals of dopaminergic neurons[58] and to inhibit AS fibrillation in vivo.[59] However, the mechanism(s) through which BS might inhibit AS aggregation are still unclear, adding more biological implications to our investigation.

In the present work, we performed a thorough spectroscopic characterization of the AS− and BS−Cu(II) complexes. Two independent, noninteracting copper-binding sites with significant differences in their binding affinities were identified in the N-terminal regions of both AS and BS. A comparative analysis of the two proteins allowed us to deconvolute the two Cu(II) binding sites along with their binding modes and affinity features. Using a mass spectrometry (MS)-based approach, we obtained unique evidence for the involvement of Met1 as the primary anchoring residue for Cu(II) in both BS and AS. A second, lower-affinity binding motif for Cu(II) is centered at position 50 in AS and 65 in BS, corresponding to the location of the sole His residue in the primary sequence of these proteins. In contrast, Cu(II) binding in the C-terminal region of synucleins represents a nonspecific, very low affinity process. Our results conclusively show that AS and BS are able to bind Cu(II) ions with affinities in the submicromolar range. This knowledge is central to an understanding of the role of Cu(II) in the fibrillization process of AS and might shed light on the molecular basis for the antiamyloidogenic effect of BS.

Experimental Section

Proteins and Reagents. Unlabeled and ^{15}N-labeled BS, AS, and truncated (1−108) AS were prepared as previously described.[4] The H65A BS and H50A AS mutants were constructed using the QuickChange site-directed mutagenesis kit (Stratagene) on BS and AS sequence-containing plasmids. The introduced modifications were further verified by DNA sequencing. Purified proteins were dialyzed

(49) Gorell, J. M.; Johnson, C. C.; Rybicki, B. A.; Peterson, E. L.; Kortsha, G. X.; Brown, G. G.; Richardson, R. J. *Neurotoxicology* **1999**, *20*, 239–247.
(50) Golts, N.; Snyder, H.; Frasier, M.; Theisler, C.; Choi, P.; Wolozin, B. *J. Biol. Chem.* **2002**, *277*, 16116–16123.
(51) Bharathi; Indi, S. S.; Rao, K. S. J. *Neurosci. Lett.* **2007**, *424*, 78–82.
(52) Bharathi; Rao, K. S. J. *Biochem. Biophys. Res. Commun.* **2007**, *359*, 115–120.
(53) Rasia, R. M.; Bertoncini, C. W.; Marsh, D.; Hoyer, W.; Cherny, D.; Zweckstetter, M.; Griesinger, C.; Jovin, T.; Fernández, C. O. *Proc. Natl. Acad. Sci. U.S.A.* **2005**, *102*, 4294–4299.
(54) Binolfi, A.; Rasia, R. M.; Bertoncini, C. W.; Ceolin, M.; Zweckstetter, M.; Griesinger, C.; Jovin, T. M.; Fernandez, C. O. *J. Am. Chem. Soc.* **2006**, *128*, 9893–9901.
(55) Bertoncini, C. W.; Rasia, R. M.; Lamberto, G. R.; Binolfi, A.; Zweckstetter, M.; Griesinger, C.; Fernandez, C. O. *J. Mol. Biol.* **2007**, *372*, 708–722.
(56) Sung, Y. H.; Eliezer, D. *J. Mol. Biol.* **2007**, *372*, 689–707.
(57) George, J. M. *Genome Biol.* **2001**, *3*, reviews3002.1−3002.6.
(58) Buchman, V. L.; Hunter, H. J.; Pinon, L. G.; Thompson, J.; Privalova, E. M.; Ninkina, N. N.; Davies, A. M. *J. Neurosci.* **1998**, *18*, 9335–9341.
(59) Hashimoto, M.; Rockenstein, E.; Mante, M.; Mallory, M.; Masliah, E. *Neuron* **2001**, *32*, 213–223.

against buffer A (20 mM MES, 100 mM NaCl, pH 6.5) or buffer B (20 mM MOPS, 100 mM NaCl, pH 7.5) supplemented with Chelex (Sigma). Protein modification with diethyl pyrocarbonate (DEPC) was performed by reacting the protein with a 5-fold molar excess of DEPC (Sigma) at room temperature for 30 min.[60] Modification yields were >95%. In some experiments, prior to DEPC modification, samples were incubated with a 10-fold molar excess of $CuSO_4$ at room temperature for 30 min. $CuSO_4$, $NiSO_4$, $MnCl_2$, $CoCl_2$, and $FeCl_2$ salts of the highest purity available were purchased from Merck or Sigma. $^{15}NH_4Cl$ and D_2O were obtained from Cambridge Isotope Laboratories (Andover, MA). Chromophoric chelator Mag-Fura-2 (MF) was obtained from Molecular Probes (Eugene, OR).

Electronic absorption, circular dichroism (CD), and NMR spectroscopy measurements were performed at 15 °C. Aggregation of 100−300 μM samples of AS in buffer A or B did not occur under these low-temperature conditions in the absence of stirring.

MALDI−TOF Mass Spectrometry. Enzymatic digestion was carried out by incubation of recombinant proteins with trypsin (Promega) in 50 mM ammonium bicarbonate, pH 6.5, for 2 h at 35 °C [enzyme/substrate ratio 1/20 (w/w)] in order to preserve *N*-carbethoxyhistidyl derivatives, which decompose at higher pH values. Digestion mixtures were further desalted using POROS 10 R2 (Applied Biosystems) homemade microcolumns. The peptides were washed with 0.1% trifluroacetic acid and then eluted directly into the mass spectrometer sample plate with 2 μL of matrix solution (α-cyano-4-hydroxycinnamic acid in 60% aqueous acetonitrile containing 0.2% trifluoroacetic acid).

Molecular masses of native and modified proteins were determined in a Voyager DE-PRO matrix-assisted laser desorption ionization−time of flight (MALDI−TOF) instrument (Applied Biosystems) equipped with a nitrogen laser (337 nm), using sinapinic acid (10 mg/mL in 50% aqueous acetonitrile containing 0.2% trifluoroacetic acid) as the matrix. External calibration was performed with cytochrome *c* as the standard. Mass spectra of digestion mixtures were acquired in a 4800 MALDI TOF/TOF instrument (Applied Biosystems) in reflector mode and were externally calibrated using a mixture of peptide standards (Applied Biosystems). In some cases, internal mass calibration was also performed using characterized peptides present in tryptic mixtures of wild-type (wt) proteins. For the identification of modified residues, collision-induced dissociation MS/MS experiments were performed.

NMR Spectroscopy. NMR spectra were acquired on a Bruker Avance II 600 MHz spectrometer using a triple-resonance probe equipped with *z*-axis self-shielded gradient coils. All of the NMR experiments were performed with pulsed-field gradient-enhanced pulse sequences on 100 μM ^{15}N-labeled protein samples in buffer A at 15 °C.

^{1}H−^{15}N heteronuclear single-quantum correlation (HSQC) amide cross-peaks affected during titrations with metal ions were identified by comparing their intensities (I) with those of the same cross-peaks (I_0) in the data set of samples lacking Cu(II). The I/I_0 ratios of 95−105 nonoverlapping cross peaks were plotted as a function of the protein sequence in order to obtain the intensity profiles. Acquisition, processing, and visualization of the spectra were performed using TOPSPIN 2.0 (Bruker), NMRPipe,[61] and Sparky, respectively.

EPR Spectroscopy. Protein samples for electron paramagnetic resonance (EPR) spectroscopy were prepared in buffer A with 50% glycerol to achieve adequate glassing. Protein concentrations were on the order of 500−700 μM. X-band EPR spectra were collected using a Bruker EMX spectrometer, ER 041 XG microwave bridge, and ER 4102ST cavity. The following conditions were used: microwave frequency, 9.4 GHz; temperature, 77 K; microwave power, 10 mW; modulation amplitude, 5 G; modulation frequency, 100 kHz; time constant, 327 ms; conversion time, 82 ms; and averaging over 12 scans. EPR spectra were baseline-corrected and simulated using WinEPR SimFonia (Bruker).

CD Spectroscopy. CD spectra were acquired with a JASCO J-800 spectrapolarimeter. Cu(II) titration experiments were performed at 15 °C on samples containing 300 μM protein in buffer A or B. A 1 cm path length cell was used to record data between 210 and 800 nm with a 2 nm sampling interval. At least five scans were recorded, and the baseline spectrum was subtracted from each spectrum. Data were expressed as difference circular dichroism ($\Delta\varepsilon$) per molar concentration of protein. To determine the affinity features of the Cu(II)−BS complex, DynaFit[62] was used to simultaneously fit changes in the CD bands in the 300−600 nm range with increasing Cu(II) concentration to a model incorporating complexes of Cu(II) in two classes of independent, noninteractive binding sites (with dissociation constants K_{d1} and K_{d2}) per protein molecule:

$$\text{Cu(II)}-\text{BS} \overset{K_{d1}}{\rightleftarrows} \text{BS} + \text{Cu(II)} \quad (1)$$

$$[\text{Cu(II)}]_2-\text{BS} \overset{K_{d2}}{\rightleftarrows} \text{Cu(II)}-\text{BS} + \text{Cu(II)} \quad (2)$$

Electronic Absorption Spectroscopy. The affinity features of Cu(II) binding to the wt species of BS and AS and their mutant forms H65A BS and H50A AS also were determined using electronic absorption spectroscopy in competition experiments involving the chromophoric metal ligand MF. Spectra were recorded at 15 °C using a JASCO V-550 spectrophotometer. The indicator MF was first titrated with Cu(II), and changes in absorbance at 363 nm with added metal were fit using DynaFit to obtain the dissociation constant of Cu(II) from its complex with MF (K_{MF}) in buffer A; a K_{MF} value of 5.0 ± 0.5 nM was obtained. Afterward, a solution of 0.5 μM MF in buffer A was titrated with Cu(II) in the presence of 5−20 μM of protein under the same experimental conditions. The changes in absorbance at 363 nm with added metal that were obtained from experiments carried out with two different protein (Syn) concentrations were fit to a model that assumed binding of 1 equiv of Cu(II) in the submicromolar range:

$$\text{Cu(II)}-\text{MF} \overset{K_{MF}}{\rightleftarrows} \text{Cu(II)} + \text{MF} \quad (3)$$

$$\text{Cu(II)}-\text{Syn} \overset{K_{d1}}{\rightleftarrows} \text{Syn} + \text{Cu(II)} \quad (4)$$

Results and Discussion

MALDI MS of DEPC-Modified and Cu(II)-Protected BS and AS: Location of the Metal-Anchoring Residues. Wild-type BS and its His mutant H65A were used to explore the feasibility of mapping copper-binding sites by protection from DEPC modification and subsequent MALDI MS analysis. To perform a comparative analysis, AS and its H50A mutant were also studied using this approach.

DEPC is a chemical that has been widely used as a protein-modification reagent that is capable of reacting with histidine residues to produce *N*-carbethoxyhistidyl derivatives. This molecule can also react with other nucleophilic residues, including cysteinyl, arginyl, and tyrosyl residues, as well with α- and ε-amino groups.[63] However, in contrast to arginine and tyrosine (BS and AS lack Cys residues, as shown in Figure 1), the imidazole ring and the α-amino groups are both known to be copper-anchoring sites. In addition, many studies have demonstrated that metal coordination to peptides or proteins protects the involved amino acids from DEPC modification.[60,64,65]

(60) Qin, K.; Yang, Y.; Mastrangelo, P.; Westaway, D. *J. Biol. Chem.* **2002**, *277*, 1981–1990.
(61) Delaglio, F.; Grzesiek, S.; Vuister, G. W.; Zhu, G.; Pfeifer, J.; Bax, A. *J. Biomol. NMR* **1995**, *6*, 277–293.
(62) Kuzmic, P. *Anal. Biochem.* **1996**, *237*, 260–273.
(63) Miles, E. W. *Methods Enzymol.* **1977**, *47*, 431–442.
(64) Fukuda, H.; Paredes, S. R.; Batlle, A. M. *Comp. Biochem. Physiol., Part B* **1988**, *91*, 285–291.

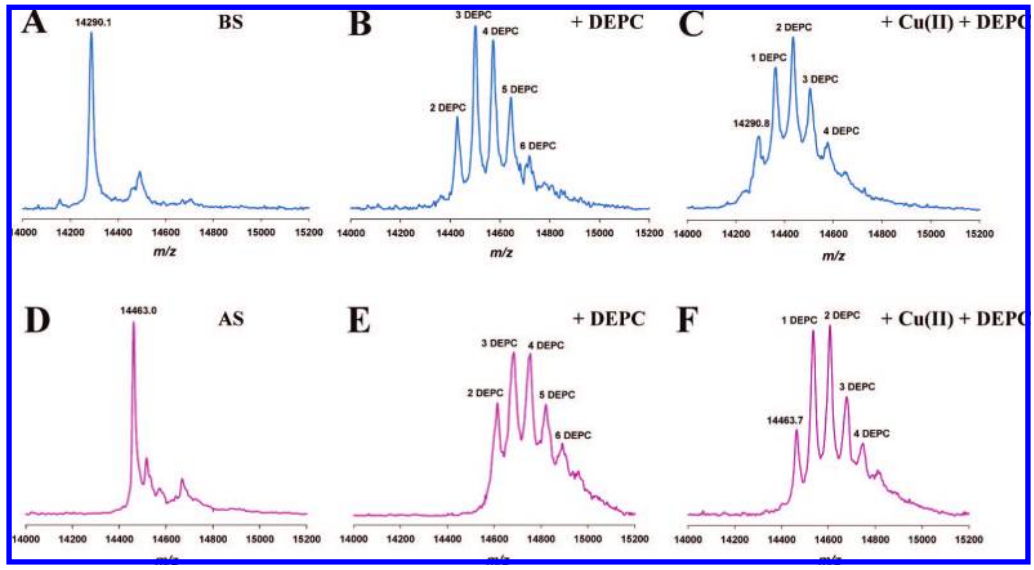

Figure 2. Effects of Cu(II) on DEPC modifications of the wt species of BS and AS. MALDI mass spectra of (A) untreated, (B) DEPC-modified, and (C) Cu(II)-protected BS and of (D) untreated, (E) DEPC-modified, and (F) Cu(II)-protected AS are shown. See the text for details.

In our studies, the proteins were incubated in buffer A with or without a 10-fold molar excess of Cu(II) for 30 min and then reacted with a 5-fold molar excess of DEPC at room temperature for 30 min prior to MALDI MS analysis.[60]

The average molecular masses [$M + H^+$] determined for the wt species of BS and AS were 14290.1 Da (calculated 14288.9) and 14463.0 Da (calculated 14461.2), respectively (Figure 2A, D). In the presence of DEPC, carbethoxylated species were detected at *m/z* 14430.2, 14501.7, 14572.3, 14643.9, and 14717.9 for BS and 14610.0, 14682.3, 14754.0, 14820.9, and 14890.9 for AS (Figure 2B,E). On the basis of a predicted mass shift of 72 Da per DEPC adduct formed, these signals were assigned to doubly, triply, quadruply, quintuply, and sextuply monocarbethoxylated products, respectively, with the most abundant ions corresponding to the incorporation of three and four modifications. A distinct modification pattern was obtained for carbethoxylated BS and AS formed after preincubation with Cu(II) (Figure 2C,F). Under these conditions, the major species were determined to be the starting wt proteins and the singly, doubly, triply, and quadruply monocarbethoxylated products, with the strongest signals corresponding to one and two modifications. These results suggest the existence of six and four sites available for DEPC modification in the untreated and Cu(II)-protected samples, respectively. The detection of mass values corresponding to the unmodified proteins in the Cu(II)-protected samples and the fact that with Cu(II) protection the largest peaks corresponded to species with one and two modifications (while the strongest signals were attributed to three and four modifications in the unprotected samples) indicate that two residues within BS and AS are protected from DEPC modification by Cu(II). Similar copper-dependent changes were observed when the experiments were performed on the C-terminal-truncated variant of AS (1−108 AS) (Figure S1A−C in the Supporting Information), indicating that the residues protected by Cu(II) coordination are located in the N-terminal region of the protein.

To determine whether His is one of the anchoring residues being protected by copper coordination, we repeated the experiments on the H65A BS (*m/z* 14222.1; calculated 14222.8) and H50A AS (*m/z* 14394.9; calculated 14395.1) mutant forms (Figure 3A,D). After incubation with DEPC, singly, doubly, triply, quadruply, and quintuply monocarbethoxylated species were observed [*m/z* 14292.6, 14365.3, 14437.1, 14509.9, and 14577.6 in H65A BS and *m/z* 14465.0, 14535.3, 14605.0, 14675.9, and 14745.9 in H50A AS (Figure 3B,E)]. These data are similar to those from the mass measurements for DEPC-derivatized species of BS and AS reacted with DEPC, except for the presence of the singly monocarbethoxylated species and the fact that only five DEPC-modified sites were observed in the mass spectra of the mutant proteins. Moreover, the maximum mass signals corresponded to double and triple monocarbethoxylation rather than to triple and quadruple monocarbethoxylation as measured for the wt species. Whereas two residues in wt BS and AS were protected from DEPC modification by Cu(II), the results in Figure 3B,C,E,F reveal that only one residue was protected by copper coordination in the H65A BS and H50A AS proteins. Altogether, these results unequivocally demonstrate that His is involved in Cu(II) binding to BS and AS.

To delimit the position of the nonhistidine copper site at the N-terminus of BS, tryptic digestion followed by MS was used to detect peptide fragments and peptide-fragment adducts in DEPC-modification and Cu(II)-protection experiments. Figure 4A−C shows the mass spectra of untreated, DEPC-modified, and Cu(II)-protected digested BS samples, respectively, in the range *m/z* 700−1600. Nine peptides (P1−P9) were detected in the resulting analysis (Table 1 in the Supporting Information). With the exception of peptides P1 and P8, no copper-dependent changes were apparent in the mass spectra of these tryptic peptides. By way of example, peaks at *m/z* values corresponding to tryptic peptides P2 (*aa* 13−21), P3 (*aa* 35−43), P4 (*aa* 33−43), P5 (*aa* 46−58), and P6 (*aa* 44−58) appeared in the mass spectra of untreated, DEPC-modified, and Cu(II)-protected digested BS (Figure 4A−C, respectively). In addition, peaks at *m/z* values corresponding to single monocarbethoxylation of peptides P7 (*aa* 35−45) and P9 (*aa* 33−45) that were not present in the mass spectra of the untreated digested samples were observed in the tryptic digestion of both DEPC-modified and Cu(II)-protected BS (Figure 4B,C, respectively). As men-

(65) Li, C.; Rosenberg, R. C. *J. Inorg. Biochem.* **1993**, *51*, 727–735.

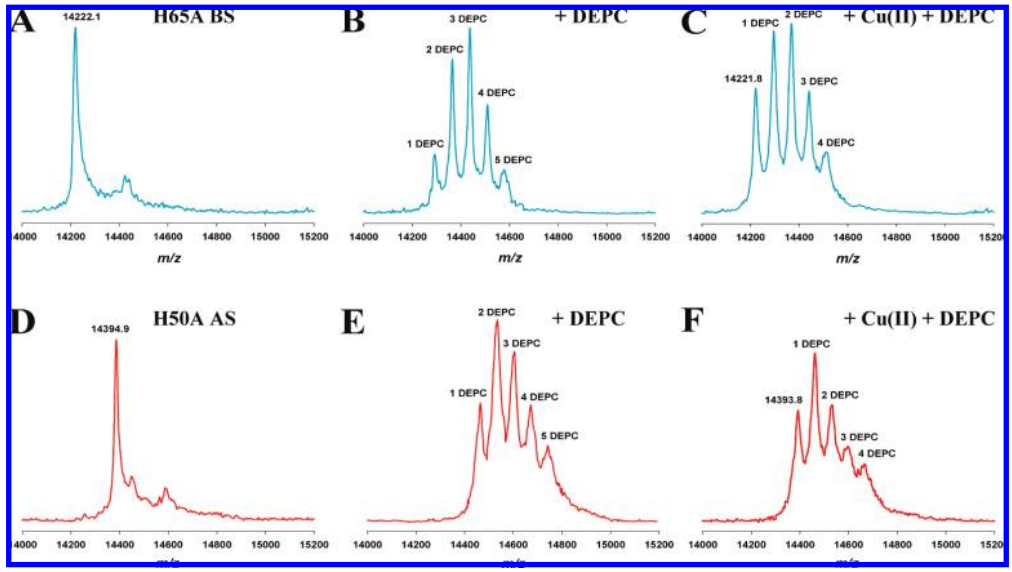

Figure 3. Effects of Cu(II) on DEPC modifications of the His mutant species of BS and AS. MALDI mass spectra of (A) untreated, (B) DEPC-modified, and (C) Cu(II)-protected H65A BS and of (D) untreated, (E) DEPC-modified, and (F) Cu(II)-protected H50A AS are shown. See the text for details.

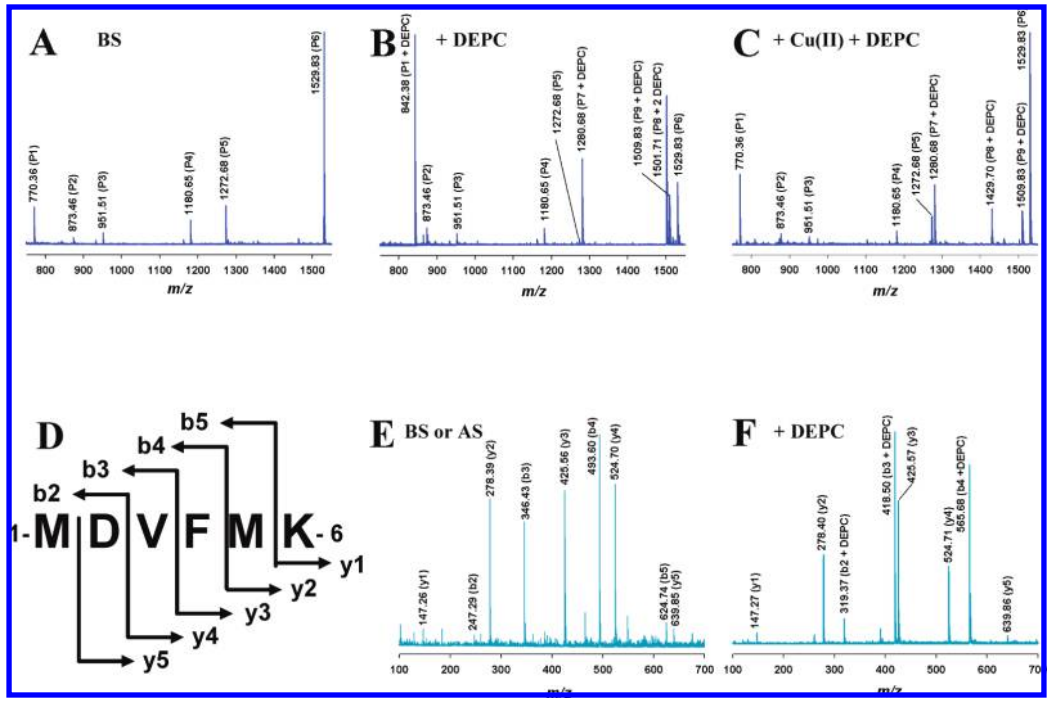

Figure 4. Mapping of the Cu(II) binding sites in BS and AS by tryptic digestion and collision-induced peptide dissociation analysis. MALDI mass spectra of the tryptic peptides obtained for (A) untreated, (B) DEPC-modified, and (C) Cu(II)-protected digested BS are shown. The *m/z* range (700−1600) excludes the His-containing tryptic peptides. Panel (D) shows a scheme for nomenclature of the ions generated by CID of the sequence ^{1}MDVFMK^{6}. N-terminal fragment ions (those containing the N-terminus of the peptide) are labeled with letter b, whereas C-terminal fragment ions (which contain the C-terminus of the peptide) are labeled with the letter y. CID mass spectra of the tryptic peptide ^{1}MDVFMK^{6} in (E) untreated and (F) DEPC-modified BS and AS samples are also shown.

tioned above, analysis of the N-terminal tryptic peptides P1 and P8 revealed a clear protective effect of copper. Tryptic peptide P1 containing the sequence ^{1}MDVFMK^{6} was detected at *m/z* 770.36 in the mass spectrum of untreated digested BS, while in the mass spectrum of the DEPC-modified digested protein, this peak was replaced with a new peak at *m/z* 842.38, corresponding to single monocarbethoxylation of P1. After Cu(II) preincubation, the peak at *m/z* 770.36 was observed again, concomitant with the disappearance of the peak at *m/z* 842.38. In the case of the tryptic fragment P8, a peak at *m/z* 1501.71 was assigned to double monocarbethoxylation of the sequence ^{1}MDVFMKGLSMAK^{12} in the mass spectrum of the DEPC-modified digested protein, indicating the existence of two sites available for DEPC modification in this peptide. When the mass spectrum of the Cu(II)-protected digested BS was analyzed, a peak at *m/z* 1429.70 corresponding to single monocarbethoxylation of the sequence ^{1}MDVFMKGLSMAK^{12} was detected, indicating that one of the two DEPC-modified sites in the P8

fragment is protected by Cu(II). Overall, these results reveal that the sequence ^{1}MDVFMK^{6} coordinates specifically to Cu(II) and protects one site in BS against DEPC modification.

Similar results were obtained when the experiments were performed on AS samples (Figure S2A−C in the Supporting Information), indicating that the sequence ^{1}MDVFMK^{6} and the His residue provide the primary binding sites for Cu(II) in this protein also.

The identification of the copper-sensitive DEPC modification site within the sequence ^{1}MDVFMK^{6} (tryptic peptide P1) was performed by collision-induced dissociation (CID) MS/MS analysis on a MALDI TOF/TOF instrument. Under these experimental conditions, fragmentation predominantly occurs at peptide-bond-generating N-terminal (b) ions and C-terminal (y) ions (Figure 4D). CID spectra of the sequence ^{1}MDVFMK^{6} and its monocarbethoxylated counterparts are shown in Figure 4E,F. The MS/MS spectrum of the singly monocarbethoxylated sequence ^{1}MDVFMK^{6} showed the presence of a complete unmodified y series (y1 to y5), whereas all of the b ions detected (b2−b5) were modified, showing the mass increment expected for singly monocarbethoxylated adducts. These results allow us to unequivocally identify Met1 as the DEPC-modified residue being protected by Cu(II) binding to the sequence ^{1}MDVFMK^{6}. Additional evidence supporting this finding arose from the analysis of the N-terminal tryptic peptide P8. In this case, two sites were available for DEPC modification in the sequence ^{1}MDVFMKGLSMAK^{12} and were identified by MS/MS analysis as Met1 and Lys6 (data not shown). Furthermore, the results clearly indicated that Lys6 is not protected by Cu(II) binding to that region. The general fact that lysine modification prevents tryptic cleavage might explain why the carbethoxylated fragment P8 was observed in the mass spectrum of DEPC-modified protein digestions but the native sequence was not detected in untreated digested protein samples. In line with many studies showing Cu(II) coordination at the N-terminal amino nitrogen of peptides and proteins,[45,66−68] our results demostrate that Met1 is the other residue directly involved in Cu(II) anchoring to BS and AS.

Finally, the addition of up to six monocarbethoxylations per protein molecule may reflect the involvement of modifications on lysine or tyrosine residues. However, in contrast with the results observed for the ^{1}MDVFMK^{6} and His-containing sequences, those residues were not protected by Cu(II) incubation, indicating that they do not participate directly in Cu(II) coordination.

NMR Mapping of the Cu(II) Complexes: N-Terminal versus C-Terminal Binding Interfaces. The details of Cu(II) binding to the studied proteins were explored at single-residue resolution by using NMR spectroscopy. A comparative analysis of the results obtained here for BS, H65A BS, and H50A AS and those reported previously for AS[53,69] was performed.

^{1}H−^{15}N HSQC NMR spectra contain one cross-peak for each amide group in the molecule (except those involving prolines) and thus provide multiple probes for locating Cu(II)-binding sites. The electron spin relaxation from the paramagnetic Cu(II) results in the differential broadening of the amide resonances linked to the paramagnetic center by through-bond or through-space interactions, providing a means of mapping metal-binding sites in the protein. We have successfully applied this strategy in the structural characterization of complexes between AS and divalent metal ions.[53,54]

A series of ^{1}H−^{15}N HSQC spectra of 100 μM BS at pH 6.5 were recorded in the presence of increasing concentrations of Cu(II) (20−60 μM) (Figure 5A−C). As in the case of AS, significant changes in cross-peak intensities occurred in the N-terminal region of BS, with the strongest broadening effects corresponding to residues 3−9 and 61−72 (residues 3−9 and 48−52 in AS were reported as being the most affected by Cu(II); see ref 53 and the inset in Figure 5F). Residues in the region 15−45 were also affected, but to a lesser extent. The I/I_0 profile of the C-terminal region revealed substantial changes only at higher Cu(II) levels, particularly in the region encompassing residues Glu121 and Glu126 (a similar trend was observed in AS[53]). NMR spectral changes induced by Cu(II) were abolished upon EDTA addition, confirming the reversibility of Cu(II) binding.[53]

The Cu(II) titration monitored by NMR showed that residues 3−9 (the amide resonances of residues 1 and 2 were not detected because of solvent-exchange effects) and those encompassing His65 in BS and His50 in AS were strongly perturbed, in line with the MALDI MS data that attributes a direct role to the α-amino group of Met1 and the imidazole ring of His as anchoring residues for Cu(II) binding to the N-terminal region of both proteins. Thus, we studied how DEPC modification affects the Cu(II)-binding features of BS. Exposure to DEPC abolished Cu(II) binding to the N-terminal region and shifted the paramagnetic influence of Cu(II) to the C-terminal region (Figure 5D), as manifested by substantial changes in cross-peak intensities at Cu(II) concentrations as low as 20 μM. Under these substoichiometric metal-to-protein conditions, the strongest effects were centered on the amide groups of Glu121 and Glu126, indicating that these residues may be the primary binding sites for Cu(II) in the C-terminal region. The Cu(II)-binding behavior monitored by NMR upon DEPC modification of BS and the presence of a coordination site formed mostly by carboxylate moieties are in agreement with a modest affinity constant (in the millimolar range) for this process, as reported for Cu(II) binding to the C-terminus of AS.[53,54] The interaction of BS with other divalent metal ions (Figure S3 in the Supporting Information) revealed that Fe(II), Mn(II), Co(II), and Ni(II) bind exclusively to the C-terminal region. Identical behavior was observed in AS,[54] demonstrating that metal binding to the highly acidic C-terminus of these proteins is a process characterized by very low selectivity and affinity.

In order to determine the implications of His replacement on the Cu(II)-binding features in the N-terminal region, the I/I_0 profile of the H65A BS mutant was measured (Figure 5E). Comparison of this I/I_0 profile to that of the wt species revealed that the changes induced by Cu(II) in the region containing the His residue were the only ones abolished upon mutation of this site, confirming that His is the anchoring residue for Cu(II) binding to this region of BS and demonstrating that the specific Cu(II) sites in the N-terminal region of the protein constitute independent motifs. Interestingly, identical behavior was observed upon mutation of His 50 in AS (Figure 5F).

The results shown in this section confirm those observed by MALDI MS and allow us to conclude that: (i) the N-terminal region of BS is the high-affinity interface for Cu(II) binding;

(66) Syme, C. D.; Nadal, R. C.; Rigby, S. E.; Viles, J. H. *J. Biol. Chem.* **2004**, *279*, 18169–18177.
(67) Wells, M. A.; Jackson, G. S.; Jones, S.; Hosszu, L. L.; Craven, C. J.; Clarke, A. R.; Collinge, J.; Waltho, J. P. *Biochem. J.* **2006**, *399*, 435–444.
(68) Balakrishnan, R.; Ramasubbu, N.; Varughese, K. I.; Parthasarathy, R. *Proc. Natl. Acad. Sci. U.S.A.* **1997**, *94*, 9620–9625.
(69) Sung, Y. H.; Rospigliosi, C.; Eliezer, D. *Biochim. Biophys. Acta* **2006**, *1764*, 5–12.

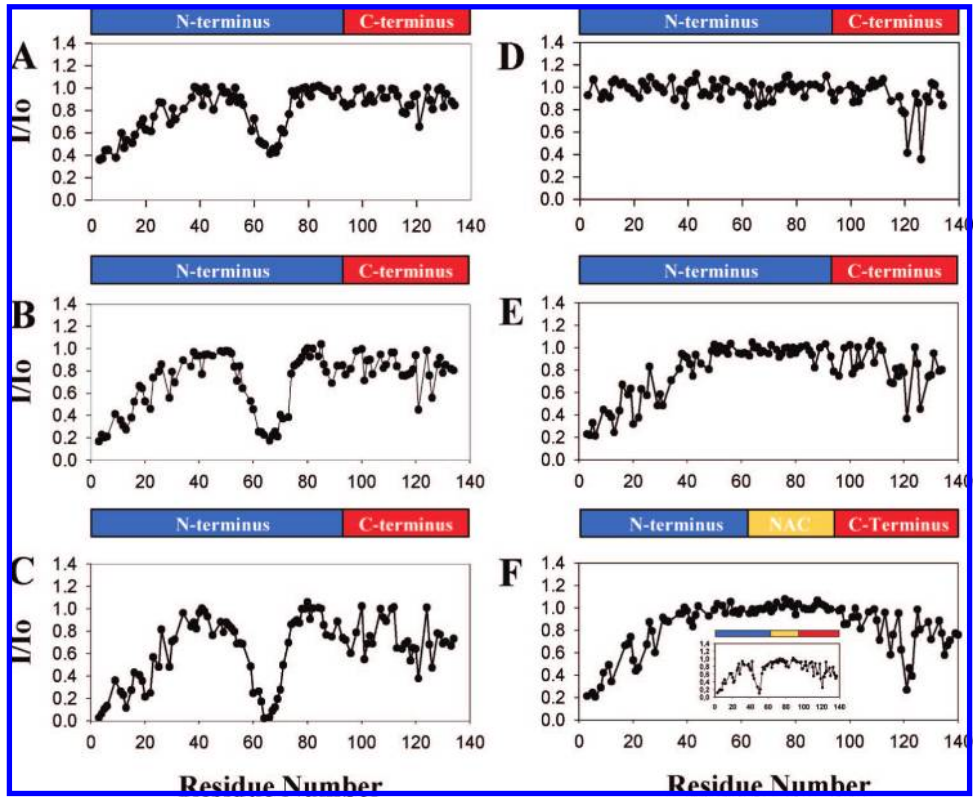

Figure 5. I/I_0 profiles of the $^1H-^{15}N$ HSQC NMR signals of the studied proteins in the presence of Cu(II). $^1H-^{15}N$ HSQC signals for 100 μM BS upon addition of (A) 20, (B) 40, and (C) 60 μM Cu(II), for (D) 100 μM DEPC-modified BS upon addition of 20 μM Cu(II), and for 100 μM (E) H65A BS and (F) H50A AS upon addition of 40 μM Cu(II) are shown. The inset in (F) displays the I/I_0 profile for 100 μM AS upon addition of 60 μM Cu(II). All of the experiments were carried out in buffer A.

(ii) the free amino group at the N-terminus and the imidazol ring of the His residue are the primary anchoring groups for Cu(II) binding to the protein; (iii) the Cu(II)-binding motifs in the N-terminal region constitute separate, independent metal-binding sites; (iv) the transient long-range interactions in AS do not influence the binding preferences of Cu(II) at each site; and (v) the binding of Cu(II) to the C-terminal region represents a very low affinity (K_d in the millimolar range), nonspecific process.

EPR Characterization of the BS−Cu(II) Complexes: Coordination Environments of the Different Metal-Binding Sites. The titration of BS with Cu(II) followed by X-band EPR at pH 6.5 is shown in Figure 6A. As reported for AS, the Cu(II) complexes of BS were also characteristic of type-2 Cu(II) proteins, with $g_{\|} \gg g_{\perp} \gg 2.0$ and large parallel hyperfine splittings, indicative of a $d_{x^2-y^2}$ ground state. At least three different Cu(II) species can be discerned from the EPR spectra on the basis of their parallel g values and hyperfine splittings. The EPR spectrum of the wt protein with 0.5 equiv of Cu(II) was dominated by a signal with a parallel hyperfine splitting (A_z) of 182 G, while a smaller amount of a second species with $A_z = 150$ G was also observed (Figure 6A, inset). Both signals grew upon further additions of Cu(II). A third species, with $A_z = 138$ G, could be distinguished from the spectra of the protein with 1.5 and 2.0 equiv of Cu(II).

In contrast to the case of the wt protein, titration of H65A BS (Figure 6B) revealed only two coordination sites for Cu(II). The EPR spectrum of the H65A protein with 0.5 equiv of Cu(II) displayed only one species, with $A_z = 182$ G (Figure 6B, inset), while the spectra of the 0.9 and 1.5 equiv samples exhibited a second species, with $A_z = 140$ G. Comparison of the 0.9 and 1.5 equiv spectra clearly showed that the higher-affinity site in the H65A protein ($A_z = 182$ G) became saturated after 1 equiv of Cu(II) was added. This was particularly evident at the lowest-field parallel hyperfine line (indicated by the arrow in Figure 6B).

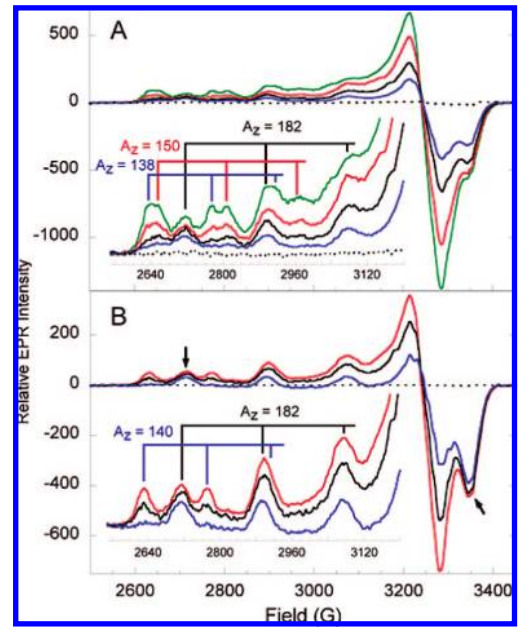

Figure 6. X-band EPR spectra of (A) wt and (B) H65A BS with (dotted black) 0, (blue) 0.5, (solid black) 0.9, (red) 1.5, and (green) 2.0 equiv of Cu(II). Spectra were collected under the conditions specified in the Experimental Section.

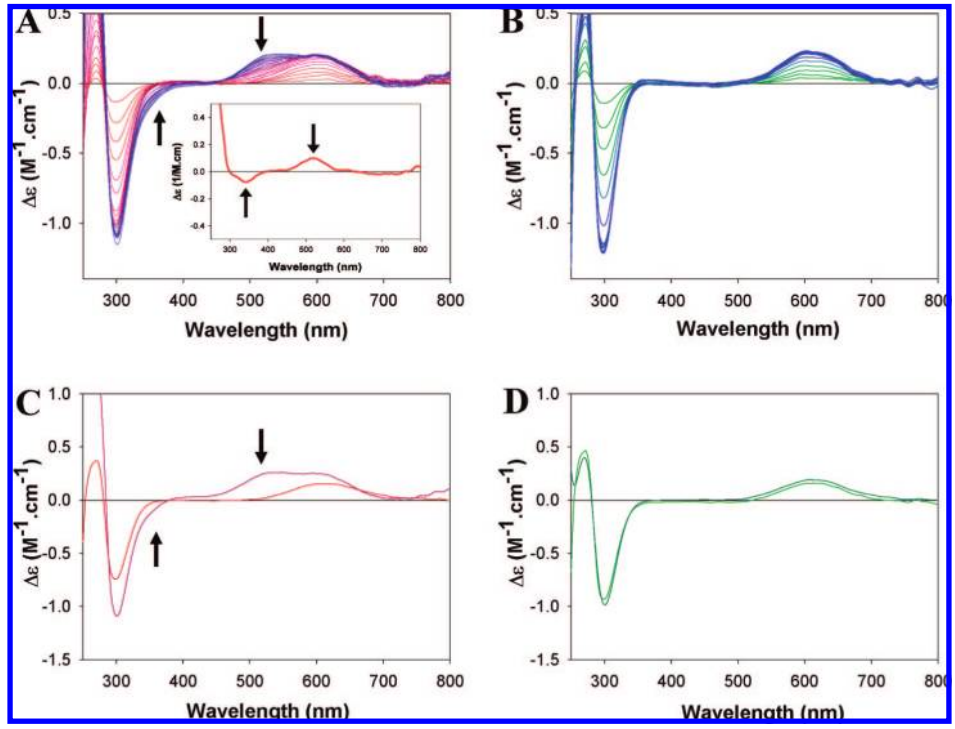

Figure 7. CD spectroscopy of BS−Cu(II) complexes. Panels (A) and (B) show the direct titration of wt and H65A BS with Cu(II), respectively. (A) Additions of 0.1 equiv of Cu(II) to wt BS as the Cu(II) concentration was incremented from (red) 0 to (blue) 3 equiv; the inset shows the differential spectra obtained by subtracting the spectrum of BS with 1 equiv of Cu(II) from that with 2 equiv. (B) Additions of 0.1 equiv of Cu(II) to H65A BS as the Cu(II) concentration was incremented from (green) 0 to (blue) 2 equiv. Panels (C) and (D) show the effect of pH on the Cu(II) complexes of wt and H65A BS, respectively. (C) BS with 2 equiv of added Cu(II) as the pH was shifted from (red) 5.0 to (purple) 6.5. (D) H65A BS with 1 equiv of added Cu(II) as the pH was shifted from (green) 5.0 to (dark-green) 6.5. In all cases, the CD spectra were acquired with 300 μM protein dissolved in buffer A (pH 5.0−6.5).

Comparison of the EPR spectra of wt and H65A BS with 0.5 equiv of Cu(II) (Figure S4A in the Supporting Information) clearly indicated that the Cu(II) coordination site with highest affinity in the wt protein is preserved upon the H65A mutation. The g_z and A_z values obtained for this high affinity site ($g_z \approx 2.250$ and $A_z = 182$ G $\equiv 191 \times 10^{-4}$ cm^{-1}) fell between the range of values associated with small Cu(II) complexes with a N_2O_2 coordination environment and the range associated with an oxygen-rich (O_4) site (Table 2 in the Supporting Information).[70,71] However, it was possible to resolve superhyperfine splittings from nitrogen in the perpendicular region of the spectrum (Figure S4A in Supporting Information), and these indicated that the coordination environment of this high-affinity site must be composed of a mixture of N- and O-based ligands. Since the Cu(II) coordination environment described for this mutant excludes the presence of His residues, it can only correspond to the site identified by MALDI MS and NMR in the sequence ^{1}MDVFMK^6. Thus, according to this model, Met1 provides one nitrogen ligand (the N-terminal NH_2 group), whereas the other nitrogen would come from the amide backbone of Asp2.[72] Although the amide resonances of Met1 and Asp2 were not detectable by NMR because of their fast exchange with the solvent, the presence of a charge-transfer (CT) band in the CD spectra of the Cu(II)−BS and Cu(II)−BS H65A complexes that was assigned to the interaction between the metal ion and a deprotonated amide group (Figure 7A,B) gives further support to this hypothesis. The oxygen ligands would most likely be provided by the carboxylate side chain of Asp2 and perhaps a water molecule.[72,73]

Figure 6 clearly shows that the second Cu(II) coordination site in wt BS, with $A_z = 150$ G, disappeared upon the H65A mutation, implicating His65 in this coordination site. The resolution of the EPR signal associated with this site was complicated by its overlap with the signal of the highest-affinity site and the appearance of a third signal after 1.5 equiv of Cu(II); however, the parallel g and A values could be resolved (Figure S4B in the Supporting Information). The g_z and A_z values obtained (2.330 and 150 G $\equiv 163 \times 10^{-4}$ cm^{-1}, respectively) for the His65 coordination suggest a NO_3 arrangement for this Cu(II)-binding site (Table 2 in the Supporting Information). His65 provides the nitrogen ligand, whereas the oxygen ligands could be provided by water molecules and/or backbone carbonyls from the peptide, although the carboxylate side chain of the proximal Glu61 cannot be discarded.

Finally, the third Cu(II) coordination site identified in the titration of the wt protein yielded a signal with $A_z = 138$ G (Figure 6A), similar to that of the second species observed in the H65A titration, for which $A_z = 140$ G (Figure 6B). The g_z and A_z values associated with the lowest-affinity Cu(II) coordination site were $g_z = 2.365$ and $A_z = 140$ G $\equiv 153 \times 10^{-4}$ cm^{-1} (Figure S4C and Table 2 in the Supporting Information). These values fell in the range of values associated with small Cu(II) complexes showing an oxygen-rich (O_4) coordination

(70) Peisach, J.; Blumberg, W. E. *Arch. Biochem. Biophys.* **1974**, *165*, 691–708.
(71) Sakaguchi, U.; Addison, W. A. *J. Chem. Soc., Dalton Trans.* **1979**, 600–608.
(72) Kallay, C.; Varnagy, K.; Micera, G.; Sanna, D.; Sovago, I. *J. Inorg. Biochem.* **2005**, *99*, 1514–1525.
(73) Kowalik-Jankowska, T.; Rajewska, A.; Wisniewska, K.; Grzonka, Z.; Jezierska, J. *J. Inorg. Biochem.* **2005**, *99*, 2282–2291.

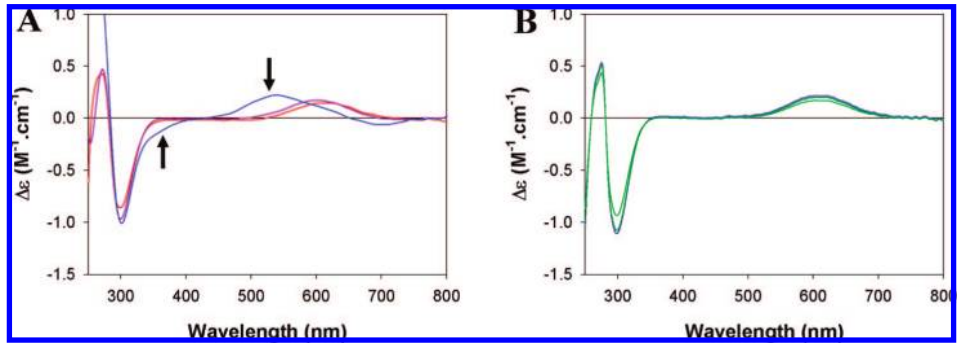

Figure 8. pH dependence of AS−Cu(II) complexes, as monitored by CD spectroscopy: (A) wt AS with 2 equiv of added Cu(II) as the pH was incremented from (red) 5.0 through (purple) 6.5 to (blue) 7.5; (B) H50A AS with 1 equiv of added Cu(II) as the pH was incremented from (green) 5.0 through (dark-green) 6.5 to (blue) 7.5. In all cases, the CD spectra were acquired with 300 μM protein dissolved in buffer A (pH 5.0−6.5) or buffer B (pH 7.5).

environment, in agreement with the binding site mapped by NMR for Cu(II) binding at the C-terminus and confirming the involvement of carboxylates as major contributors to metal binding in this region.[70,71]

Cu(II)-Binding Affinity of BS− and AS−Cu(II) Complexes As Determined by Absorption and CD Spectroscopy. 1. CD Analysis of Cu(II) Complexes. To ascertain the binding-affinity features of the BS−Cu(II) and AS−Cu(II) complexes, we first recorded the CD spectra of BS with increasing concentrations of added Cu(II) (Figure 7). At substoichiometric Cu(II)/BS ratios, the CD spectra of the BS−Cu(II) complex at pH 6.5 strongly resembled those reported for AS,[53] showing a positive band in the d−d region (~600 nm) and a negative CT band at 300 nm (Figure 7A). Beyond 1 equiv of Cu(II), two additional bands were evident at 520 and 340 nm (indicated by the arrows in Figure 7A and its inset), both of which saturated with 2 equiv of added Cu(II). Interestingly, the latter bands were not detected in the CD spectra of AS−Cu(II) complexes recorded under similar experimental conditions (Figure 8A and ref 53). When the same studies were performed on the H65A variant of BS, only the bands at 600 and 300 nm remained in the CD spectra, and they saturated with 1 equiv of added Cu(II) (Figure 7B). Since the CD spectra of H65A BS complexed with Cu(II) lacked the bands at 520 and 340 nm, these bands must correspond to the BS−Cu(II) complex in which His65 acts as the main anchoring residue. The band at 340 nm is attributed to a CT transition between the metal center and an imidazole group (π_1 N_{im}−Cu CT, 280−345 nm), which is typical of His−Cu(II) complexes.[73,74] Accordingly, the positive band at 600 nm and the negative band at 300 nm reflect the coordination of Cu(II) to the high-affinity binding site of BS. The band at 300 nm is assigned to a CT transition between the metal center and a deprotonated peptide nitrogen [(N^-)−Cu CT, 295−315 nm].[72−74]

Interestingly, the CD spectra recorded for DEPC-treated BS and AS samples showed no signals upon addition of Cu(II). Moreover, the CD spectrum of Cu(II) bound to the C-terminal-truncated variant 1−108 AS (Figure S5 in the Supporting Information) was identical to that recorded for AS.[53] These results indicate that under our experimental conditions, the CD spectra of BS−Cu(II) and AS−Cu(II) complexes report exclusively on Cu(II) binding to the N-terminal region.

In order to gain further insights into the spectral differences found for the AS− and BS−Cu(II) complexes, we also monitored the effect of pH. The CD spectrum acquired at pH 5.0 for BS−Cu(II) with 2 equiv of Cu(II) added contained a positive CD band at ~600 nm (Figure 7C) and was similar to the spectrum obtained at pH 6.5 with only 1 equiv of Cu(II) added. When the pH was increased to 6.5, the additional band centered at 520 nm (indicated by an arrow in Figure 7C) became evident again in the visible region of the CD spectrum. These spectral features were not observed when the pH dependence of the H65A BS variant complexed with Cu(II) was studied (Figure 7D), and therefore, these spectral changes were attributed to the environment of the His65−Cu(II) complex. Further supporting evidence comes from the pH-dependent behavior of the CT band at 340 nm (labeled by an arrow in Figure 7C), which corresponds to the imidazol ring of His65.

We have reported previously that the CD spectrum of AS complexed with 1 equiv of Cu(II) in buffer A at pH 6.5 was characterized by the presence of a positive d−d band at 600 nm and a negative CT band at 300 nm.[53] Whereas the CD band at 300 nm saturated with 1 equiv of Cu(II), the intensity of the CD band at 600 nm decreased as the amount of Cu(II) increased from 1 to 2 equiv and then remained constant at higher Cu(II) concentrations. The decrease in ellipticity at 600 nm observed beyond 1 equiv of Cu(II) was attributed to the development of a negative contribution associated with formation of the second Cu(II) complex. This suggestion was confirmed here by recording the CD spectra of AS complexed with Cu(II) (2 equiv added) in the pH range 5.0−7.5. As shown by the arrows in Figure 8A and Figure S6A,C in the Supporting Information, the spectrum recorded at pH 7.5 clearly shows the presence of a positive band at 520 nm and the development of a negative ellipticity that overlaps with the CD band in the 600 nm region, likely reflecting coordination features of the Cu(II)−His50 complex in AS. The detection of the CT band at 340 nm (π_1 N_{im}−Cu CT) in the spectrum at pH 7.5 (marked with arrows in Figure 8A and Figure S6A,C), together with the absence of such pH-dependent behavior in the CD spectrum of AS H50A complexed to Cu(II) (Figure 8B) gives further support to our conclusions. Since histidine residues are involved in Cu(II) coordination to AS and BS, one could postulate that the titratable imidazole side-chain of histidines might be the main source of the differences observed in the CD spectra of the two proteins in the pH range analyzed.

2. Binding Affinity. Once we assigned the CD bands to specific Cu(II) complexes in the protein, we intended to estimate the metal-binding affinity of each site. Fine titration of wt BS with Cu(II) was followed by CD spectroscopy in order to monitor the buildup of the CT band (300 nm) and the d−d bands (520 and 600 nm) (Figure 9A). The spectroscopic changes upon

(74) Daniele, P. G.; Prenesti, E.; Ostacoli, G. *J. Chem. Soc., Dalton Trans.* **1996**, 3269–3275.

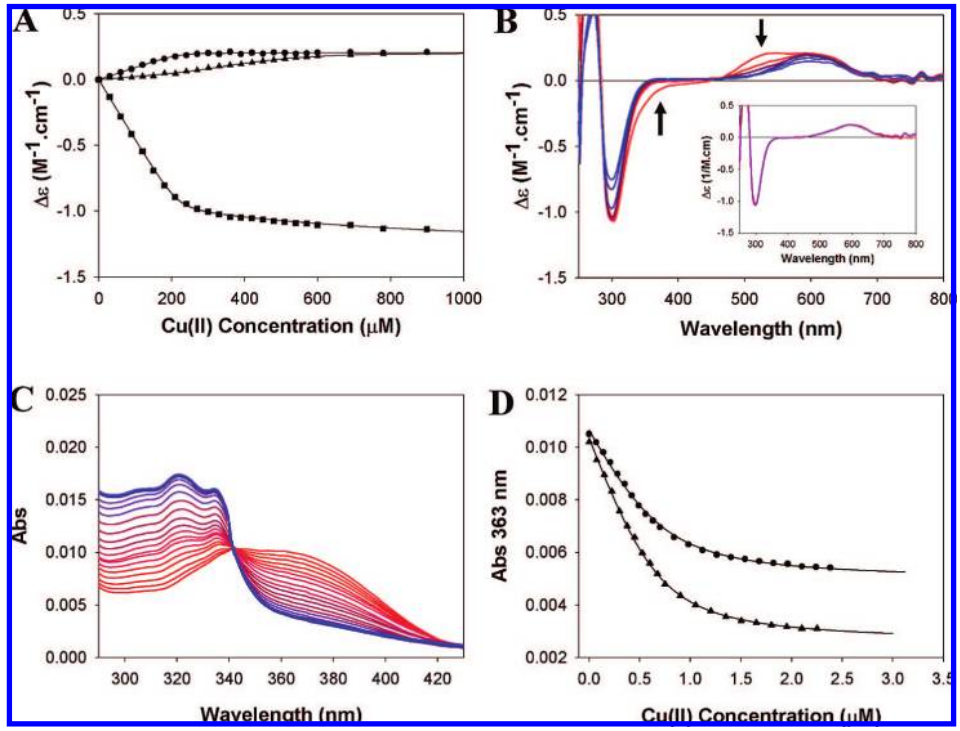

Figure 9. Determination of the affinities of the BS−Cu(II) complexes at pH 6.5. (A) Direct titration of BS with Cu(II) monitored by CD spectroscopy: binding curves at 600 (●), 520 (▲), and 300 nm (■) are plotted as functions of the amount of Cu(II) added; the solid lines correspond to fits of the experimental data according to eqs 1 and 2 in the Experimental Section. (B) Cu(II) affinity for BS from glycine competition, monitored by visible CD spectroscopy: spectra of BS with 2 equiv of Cu(II) as the Gly concentration was incremented from 0 to 12 equiv are displayed (the red-to-blue spectral progression corresponds to addition of 0, 1, 2, 4, 8, and 12 equiv of Gly); the inset shows the spectrum of BS with 1 equiv of added Cu(II) overlaid with that of BS with 2 equiv of added Cu(II) in the presence of 2 equiv of Gly. (C) Cu(II) affinity for BS from MF competition, monitored by electronic absorption spectroscopy: titration of a solution containing 0.5 μM MF and 5 μM wt BS in buffer A are shown (the red-to-blue progression corresponds to increasing Cu(II) concentration). (D) Absorbance changes at 363 nm from two independent MF competition experiments: curves for 5 μM BS (▲) and 15 μM BS (●) are shown; the solid lines correspond to fits of the experimental data according to eqs 3 and 4 in the Experimental Section, resulting in a dissociation constant for the BS−Cu(II) complex of $K_{d1} = 0.2 \pm 0.02$ μM.

Cu(II) addition at 300, 520, and 600 nm were fit to a model that assumed binding of 2 equiv of Cu(II) in the submicromolar-to-micromolar range (eqs 1 and 2 in the Experimental Section). From this experiment, we estimated the following values of the macroscopic dissociation constants: $K_{d1} = 0.7 \pm 0.6$ μM and $K_{d2} = 60 \pm 20$ μM, in full agreement with the values reported previously for the binding of Cu(II) to the N-terminal region of AS on the basis of electronic absorption spectroscopy.[53] Analyses for the BS H65A and AS H50A species that assumed the binding of 1 equiv of Cu(II) in the submicromolar range yielded K_{d1} values of 0.3 ± 0.4 and 0.6 ± 0.6 μM, respectively (data not shown). Despite the large numerical uncertainties associated with these quantities, which are due to the high concentration of the protein required to achieve accurately measurable signals ($[AS]_{tot} \gg K_{d1,2}$), their relative order of magnitude was well-established.

The affinity features in the N-terminal region were further confirmed by using glycine as a copper competitor. Two glycine molecules can bind to one Cu(II) with an apparent K_d of ~10 μM (pH 6.5) via both the amino and carboxylate groups.[66] The resulting $Cu(Gly)_2$ visible absorption bands are CD-silent. Figure 9B shows the CD spectrum for BS with 2 equiv of Cu(II) at pH 6.5 as the protein is titrated with glycine. If glycine had been able to successfully compete with BS for Cu(II) ions, then 4 equiv of glycine would be sufficient to remove both Cu(II) ions from the protein. Addition of increasing amounts of glycine gradually decreased the intensity of the CD bands at 340 and 520 nm (arrows in Figure 9B), corresponding to the Cu(II) complex involving His65. After the addition of 2 equiv of glycine, the CD spectrum was identical to that recorded for BS with only one equivalent of Cu(II) added (Figure 9B, inset), indicating that glycine was able to successfully remove the copper atom bound to the His site. Subsequent additions of glycine up to a total of 8 equiv did not perturb the CD bands at 300 and 600 nm, confirming the affinity ranges estimated by CD titration experiments and indicating that the affinity of the Cu(II) complexes decrease in the order α-NH_2−Cu(II) site > His−Cu(II) site. A competition experiment carried out on AS at pH 7.5 supported the affinity order determined for the Cu(II) binding sites in BS (see the arrows in Figure S7 in the Supporting Information).

Finally, in order to obtain more reliable K_{d1} values for the strongly bound Cu(II) ion, we performed competition experiments involving the chromophoric metal ligand MF, whose spectroscopic features change upon Cu(II) binding. This procedure has been employed to monitor Zn(II), Cd(II), and Co(II) binding to metalloproteins.[75,76] The titration data for the chelator MF with Cu(II) ions are shown in Figure S8 in the Supporting Information, from which a value of 5.0 ± 0.5 nM was estimated for K_{MF}, the dissociation constant for the Cu(II)−MF complex. The spectra showed an isosbestic point at 340 nm and maxima at 363 and 320 nm for the metal-free compound and the 1:1 Cu(II) complex, respectively. The titration data measured for

(75) de Seny, D.; Heinz, U.; Wommer, S.; Kiefer, M.; Meyer-Klaucke, W.; Galleni, M.; Frere, J. M.; Bauer, R.; Adolph, H. W. *J. Biol. Chem.* **2001**, *276*, 45065–45078.
(76) Llarrull, L. I.; Tioni, M. F.; Kowalski, J.; Bennett, B.; Vila, A. J. *J. Biol. Chem.* **2007**, *282*, 30586–30595.

BS are shown in Figure 9C,D. By considering the model represented by eqs 3 and 4 in the Experimental Section, a submicromolar dissociation constant was obtained for the first equivalent of Cu(II) bound to the protein ($K_{d1} = 0.20 \pm 0.02$ μM). Similar values were obtained when the experiments were performed on wt AS and the variants BS H65A and AS H50A (data not shown).

Altogether, these results indicate that BS and AS bind Cu(II) ions with similar affinities and that complexation through the α-amino group of Met1 represents the highest-affinity event in Cu(II) binding to both BS and AS.

Conclusions

The structural characterization of Cu(II) binding to BS is reported here for the first time and compared with AS in order to address unresolved structural details related to the specificity of Cu(II) binding. Two independent, noninteracting copper-binding sites were detected in the N-terminal region of AS and BS. Using an MS-based approach, we have unequivocally demonstrated the direct role of Met1 as the primary anchoring residue for Cu(II) in both proteins. From the binding features of the Cu(II) complexes studied, we can draw the following conclusions: (i) the high-affinity Cu(II)-binding site in AS and BS ($K_d = 0.20 \pm 0.02$ μM) is the one in which the N-terminal amino nitrogen of Met1 acts as the anchoring group and Asp2 and a water molecule are suggested to also be involved in the ligand donor set;[73] (ii) a second lower-affinity binding motif for Cu(II) ($K_d \approx 50$ μM) is centered at position 50 in AS and 65 in BS, corresponding to the location of the sole His residue in the primary sequence of these proteins; and (iii) AS and BS bind metal ions to the C-terminus with very low selectivity (K_d in the millimolar range), where carboxylates of Glu/Asp121 and Glu126 act as major contributors to the binding process.

New insights into the bioinorganic chemistry of Parkinson's disease are implied by these findings. As mentioned before, Cu(II) has been implicated in the pathogenesis of age-dependent degenerative diseases characterized by deposition of amyloid material. Interestingly, the affinity of Cu(II) for the target proteins involved in several of these diseases is in the low or submicromolar range. Thus, the fact that AS binds Cu(II) with an affinity in the submicromolar range and that Cu(II) can efficiently promote AS aggregation at physiologically relevant concentrations establish a tight link with other amyloid-related disorders, such as Alzheimer's disease and prion disease, and support the notion of PD as a metal-associated neurodegenerative disorder.

In regard to the possible role played by His in the Cu(II)-mediated aggregation of AS, our results indicate that the effect of Cu(II) concentration on AS aggregation in vitro, at least for the earliest aggregational events, seems to be related neither to specific histidine binding nor to the general factors usually invoked for AS aggregation, such as the interaction with clusters of negatively charged residues at the C-terminal region. Supporting this possibility is the absence of any interplay or modulation among the identified Cu(II)-binding sites of the wt species. Thus, we could hypothesize that copper binding to the high-affinity site of AS might be the critical step in rendering the protein a relatively easy target for destabilization, a process that in vivo might lead to a cascade of subsequent structural alterations promoting the generation of a pool of AS molecules that are more prone to aggregate.

Finally, the evidence presented in this work might also explain the preventive effect of BS on AS aggregation. β-Synuclein, the nonamyloidogenic AS homologue that naturally lacks the NAC domain, was shown to be colocalized with AS at the presynaptic terminals of dopaminergic neurons and to inhibit its aggregation in vivo.[59] Although the mechanism by which BS might inhibit AS aggregation is unclear, several possibilities might be considered. For example, BS might directly bind to AS and prevent further aggregation, but a recent study showed that no interaction takes place between the two proteins in vitro.[56] On the other hand, our study supports the idea that the BS inhibitory effect might be related to the comparable affinities for copper in the two proteins. Thus, the simplest hypothesis might be that BS also acts as a copper-sequestering protein, playing the role of a copper sponge and thereby preventing or attenuating the subsequent oligomerization of AS.

Acknowledgment. C.O.F. thanks ANPCyT, Fundacion Antorchas, CONICET, the Max Planck Society, and the Alexander von Humboldt Foundation for financial support. C.O.F. is the head of a Partner Group of the Max Planck Institute for Biophysical Chemistry (Göttingen). A.B. and G.R.L. are recipients of a fellowship from CONICET in Argentina. R.D. and C.C. thank Magdalena Portela for her helpful technical assistance. L.Q. thanks Consejo Nacional de Ciencia y Tecnología (CONACYT, Project J48781Q) and the National Fellowship for Women in Science L'Oreal-UNESCO 2007. C.W.B. is the recipient of an EMBO long-term fellowship. M.Z. is supported by a DFG Heisenberg scholarship (ZW 71/2-1 and 3-1). The authors thank Dr. Leticia I. Llarrull and Prof. Edward I. Solomon (Stanford University) for useful discussions and Prof. Thomas Jovin and Ms. Ritika Mahal for initial support and work on the characterization of metal-ion binding to BS.

Supporting Information Available: Tables containing MALDI MS and EPR data for BS−Cu(II) complexes, MALDI MS spectra of 1−108 AS, NMR I/I_0 profiles for the various BS−metal(II) complexes, EPR and CD spectra of AS− and BS−Cu(II) complexes under different experimental conditions, results of a Cu(II) titration of MF followed by electronic absorption spectroscopy, and complete ref 31. This material is available free of charge via the Internet at http://pubs.acs.org.

JA803494V